Global Flexible Power Point Tracking in Photovoltaic Systems Under Partial Shading Conditions

Hossein Dehghani Tafti, *Senior Member, IEEE*, Qijun Wang, Christopher D. Townsend, *Member, IEEE*, Josep Pou, *Fellow, IEEE*, and Georgios Konstantinou, *Senior Member, IEEE*

***Abstract*—Flexible power point tracking (FPPT) aims to regulate the output power of photovoltaic (PV) systems to a predefined value to enable grid support functionalities, such as virtual-inertia provision. Even though partial shading is a common condition in PV systems, especially in small-scale residential PV systems, the current literature, only investigates FPPT control under uniform shading conditions. This article proposes a novel global FPPT (GFPPT) algorithm to provide two functionalities in PV systems under partial shading conditions: first, constant power control (CPC), in which the PV power is regulated to predefined reference value, and second, power reserve control (PRC), under which a constant power reserve is kept in the PV system under steady state to enable grid support under transients. The conventional global maximum power point tracking (GMPPT) algorithm is also modified to adapt with the proposed GFPPT algorithm. The aim of such modification is to obtain faster dynamics after the detection of any environmental changes. Experimental results under dynamically changing partial shading conditions verify the effectiveness of the proposed algorithm in providing CPC or PRC functionalities in PV systems.**

***Index Terms*—Active power control, flexible power point tracking (FPPT), frequency support, global maximum power point tracking (GMPPT), inertia provision, partial shading.**

I. Introduction

MAXIMUM power point tracking (MPPT) algorithms are conventionally used in photovoltaic (PV) systems to maximize the available output power in these systems [1]. Several MPPT algorithms are introduced in the literature with different features such as low-power oscillations at steady state or fast dynamics [2]–[4]. Some of these MPPT algorithms are mainly applicable under uniform shading in PV strings. However, partial shading occurs frequently in PV systems, especially in small-scale rooftop PV systems due to passing clouds or unavoidable shading during certain hours of the day. Accordingly, several algorithms are introduced in the literature to enable PV systems with global maximum power point tracking (GMPPT). Table I summarizes some of the available MPPT algorithms under uniform and partial shading conditions. High penetration of renewable energy resources, especially PV systems, leads to new challenges in operation and management of power systems, such as reduced inertia or reverse power flow. Replacement of conventional synchronous generators with converter-based distributed generation (DG) systems leads to the reduction of available inertia in power systems. Synchronous generators have inertia due to rotating mechanical rotor, but such inertia does not exist in conventional converter-based DGs. Additionally, the power generated with DGs in downstream of the power system can flow toward upstream buses (referred as reverse power flow), leading to over voltage in downstream buses [5], [6].

New requirements such as frequency response, power ramp rate limit, and Volt–Watt ($P(V)$), are mandated by new standards to maintain the security and reliability of the power system with high penetration of PV systems [7], [8]. Accordingly, flexible power point tracking (FPPT) algorithms are required in PV systems, to regulate the PV power to the required reference value, based on the corresponding standard and grid operating conditions [9]. The principles of FPPT control under uniform shading are illustrated in Fig. 1(a). The operation point, instead of being at maximum power point (MPP), moves to the right- or left-side of the MPP, corresponding to the power reference p_{fpp}. Similarly, under partial shading condition, the operation point instead of being at the global maximum power point (GMPP), moves to one of the shown points corresponding to p_{fpp} in Fig. 1(b). This operation controlled is referred as global flexible power point tracking (GFPPT) in this article.

As an example, one of the required grid support functionalities, based on the new standards is frequency–Watt ($P(f)$) response [7], [8], which necessitates GFPPT control in PV systems. It should be noted that other grid support functions, such as low-voltage ride through capability, Volt–VAr ($Q(V)$), etc., also require GFPPT operation of PV systems. The $P(f)$ response, required for PV systems is illustrated in Fig. 2. Accordingly, the

Manuscript received November 21, 2021; revised March 12, 2022; accepted April 8, 2022. Date of publication April 19, 2022; date of current version May 23, 2022. This work was supported by the Future Battery Industries Cooperative Research Centre as part of the Australian Government's CRC Program, which supports industry-led collaborations between industry, researchers, and the community. Recommended for publication by Associate Editor Y. Li. *(Corresponding author: Hossein Dehghani Tafti.)*

Hossein Dehghani Tafti and Christopher D. Townsend are with the Department of Electrical, Electronic and Computer Engineering, University of Western Australia, Crawley, WA 6009, Australia (e-mail: hossein002@e.ntu.edu.sg; townsend@ieee.org).

Qijun Wang and Georgios Konstantinou are with the School of Electrical Engineering and Telecommunications, University of New South Wales, Sydney, NSW 2052, Australia (e-mail: qijun.wang@student.unsw.edu.au; g.konstantinou@unsw.edu.au).

Josep Pou is with the School of Electrical and Electronic Engineering, Nanyang Technological University, Singapore 639798 (e-mail: josep.pou@ieee.org).

Color versions of one or more figures in this article are available at https://doi.org/10.1109/TPEL.2022.3167657.

Digital Object Identifier 10.1109/TPEL.2022.3167657

TABLE I
OVERVIEW OF AVAILABLE FPPT ALGORITHMS IN THE LITERATURE

	MPPT	**FPPT**
Uniform Shading	• Perturb & observe [10]–[12] • Incremental conductance [13], [14] • Fractional short circuit current / open circuit voltage [15], [16] • Kalman filter [17] • Fuzzy logic control [18], [19] • Ant colony optimization [20] • Hil climbing method [21] • Beta parameter approach [22] • MPP Locus characterization approach [23] • . . .	• Modified converter controller – Direct power control [24], [25] – Multi-mode with PV voltage control [26], [27] – PV power-based delta-voltage control [28] – Direct voltage reference calculation • Direct voltage reference calculation – Constant voltage step-based P&O [26], [29]–[31] – Adaptive voltage step-based P&O [32]–[34] – Non-linear search [35], [36] • . . .
Partial Shading	• Modified incremental conductance [37], [38] • Particle swarm optimization [1], [39] • Modified cat swarm optimization [40] • Grey wolf optimization [41] • Hybrid algorithms [42] • Cuckoo search algorithm [43], [44] • Search-skip-judge [45] • . . .	• Curve fitting-based control algorithm [46] • Deloading-based power reserve control [47] • HC&PSO-based FPPT algorithm [48] • ***??? (A computationally simple and general GFPPT algorithm that is applicable to multiple PV module systems)***

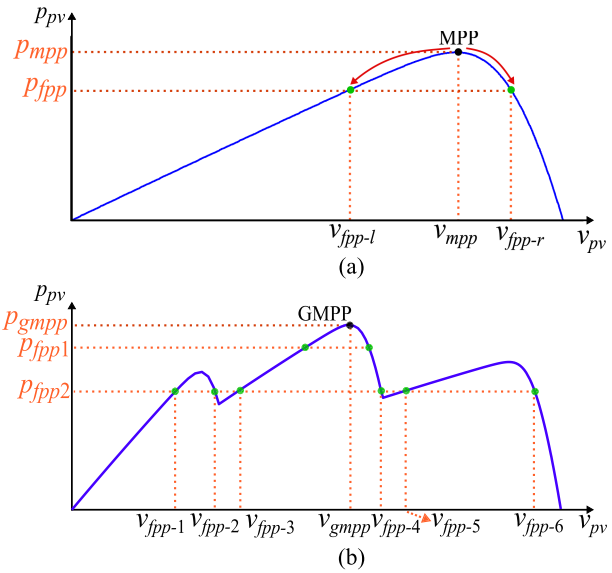

Fig. 1. Principle of flexible power point tracking under: (a) Uniform shading, and (b) partial shading conditions.

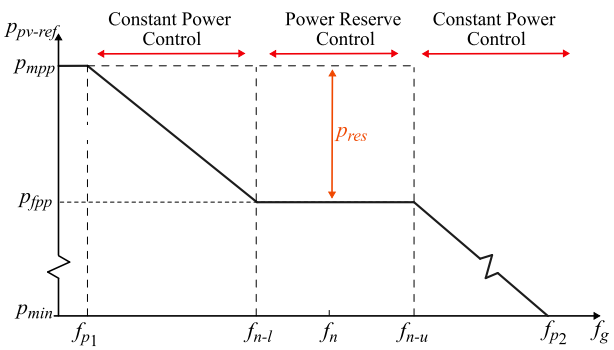

Fig. 2. Grid frequency support through $P(f)$ curve.

operation mode of the PV system is classified into the following two modes.

1) *Power reserve control (PRC):* This operation mode is activated while the grid frequency (f_g) is within its nominal range ($f_{n-l} < f_g < f_{n-h}$), as shown in Fig. 2. Under this operation mode, a constant amount of power reserve p_{res} is kept in the PV system. The available maximum PV power should be known under this operation mode, to ensure the required amount of power reserve in the system.
2) *Constant power control (CPC):* The power reference is calculated using the $P(f)$ droop curve under this operation mode, as illustrated in Fig. 2. This operation mode is enabled under frequency disturbance conditions. Accordingly, the PV power is regulated to this reference value.

Various FPPT algorithms are available in the literature to satisfy these operation modes. Based on the solution for regulating the power to a reference value, these algorithms can be classified into two categories [9].

1) *Modified converter controller:* In this category of FPPT algorithms, the PV power regulation is achieved by modifying the controller of the dc–dc converter in two-stage PV systems or the inverter in single-stage PV systems. The PV voltage reference is calculated using an MPPT algorithm and is modified in the controller to regulate the PV power. Several algorithms are available in the literature under this category, which are listed in Table I.
2) *Direct voltage reference calculation:* The FPPT algorithms under this category directly calculate the voltage reference corresponding to the power reference. A conventional control strategy is used to regulate the PV voltage to the calculated reference value. These algorithms either use a linear [26], [29]–[34] or nonlinear search [35], [36] to find the PV voltage reference.

As shown in Table I, currently, there are very few solutions in the literature for the FPPT control of PV systems under partial

shading conditions. An active PRC through curve fitting is proposed in [46] under partial shading conditions. This algorithm necessitates frequent scanning of the PV curve for different PV modules. To avoid this repeated scanning, a power control strategy based on deloading of the PV power is presented in [47]. The deloading region is chosen according to the GMPP, whether it happens in the right-, left-, or middle-side of the PV curve. The voltage reference for scanning the curve is also generated based upon the number of shaded and unshaded modules in the array. Despite the effectiveness of this solution for PV arrays with two PV modules, the algorithm becomes complex for PV arrays with multiple PV modules and typically there are more than two LMPPs in the PV curve in practical applications. Furthermore, if the power reference is smaller than the power of the section divider point in the PV curve, the algorithm may not be able to regulate the power accurately. To increase the convergence rate, an optimization-based FPPT is proposed in [48]. It uses hill-climbing and particle swarm optimization algorithm (HC&PSO)-based FPPT algorithm. However, the computational complexity of implementation of the optimization process reduces the interest for practical systems. Accordingly, to the best of the knowledge of the authors, there is no computationally simple and general FPPT algorithm in the literature under partial shading conditions that can work effectively with multiple PV module systems.

To fill the research gap, this article proposes an GFPPT algorithm under partial shading conditions, to satisfy the two mentioned required functionalities: i) CPC and ii) PRC. The combination of the two algorithms equips PV systems with grid frequency support, under all possible irradiance conditions. The main advantage of the proposed algorithm, compared to the state-of-the-art is its applicability for both constant power and PRC scenarios. Another advantage of the proposed solution is its applicability to PV arrays with any number of local MPP points. Additionally, the proposed solution does not use any intelligent- or optimization-based algorithms, which reduces its implementation complexity and provides computational superiority, compared to the available solutions, in practical systems. To find the GMPP under partial shading conditions, a conventional search-skip-jump GMPPT algorithm [45] is modified to be compatible with the proposed GFPPT algorithm. Experimental tests verify the effectiveness of the proposed algorithms under dynamically changing partial shading conditions in providing either a constant power generation or PRC functions in PV systems.

The rest of this article is organized as follows. The details of the proposed GFPPT algorithms under partial shading conditions are provided in Section II. Experimental results under dynamically changing partial shading conditions are provided in Section III. Finally, Section V concludes this article.

II. Proposed GFPPT Algorithms Under Partial Shading Conditions

Details of the proposed GFPPT algorithms are provided in this section. First, an overview of the PV system and control structure is provided. Subsequently, the proposed GFPPT algorithm with CPC functionality is explained. Finally, details of the proposed GFPPT algorithm with PRC are elaborated.

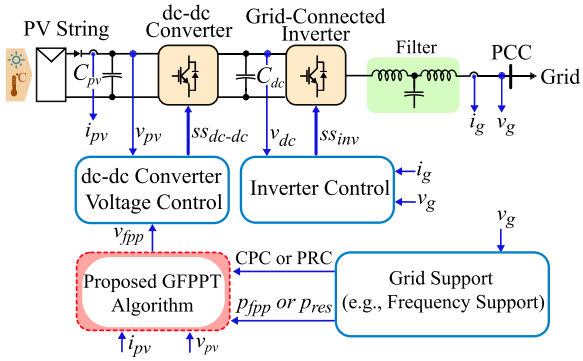

Fig. 3. Overview of a two-stage PV system with the proposed GFPPT algorithm under partial shading conditions.

A. System Description

An overview of a two-stage PV system and its overall control overview is illustrated in Fig. 3. A conventional inverter controller is implemented to regulate the dc-link voltage $v_{\rm dc}$ to its reference value and inject the extracted power from the PV string to the grid [34]. The grid support block first detects the operation mode to be CPC or PRC based on the grid operating condition (steady-state or transient). It also calculates the required power reference $p_{\rm fpp}$ or power reserve $p_{\rm res}$, based on the grid frequency. As an example, "grid support" in [49] and [50] provides frequency support by keeping a power reserve during steady-state operation (PRC functionality) and regulating the PV power based on $P(f)$ droop during frequency disturbance conditions (CPC functionality). Based on the required power reference $p_{\rm fpp}$ or power reserve $p_{\rm res}$, the proposed GFPPT algorithm calculates the corresponding PV voltage references $v_{\rm fpp}$. The details of this block are provided in the following sections. A conventional controller is also implemented to regulate the PV voltage $v_{\rm pv}$ to its reference value [34]. It is noted that the proposed algorithm can also be applied to single-stage PV systems. In this case, the proposed GFPPT algorithm calculates the voltage reference for the dc-link of the inverter. A conventional controller can be applied to regulate the dc-link voltage of the inverter to the calculated voltage reference by the GFPPT algorithm.

B. Proposed GFPPT Algorithm With CPC Functionality

The input to the GFPPT algorithm with CPC functionality is the PV power reference $p_{\rm fpp}$, as shown in Fig. 3. The principle of the CPC operation is illustrated in Fig. 4. In this case, the PV curve has two intersection points with the $p_{\rm fpp}$ line, points ① and ②. If the current operation point is larger than the power reference [shown in Fig. 4(a)], the PV power needs to be reduced toward the power reference. To attain a fast response, it is noted that if the slope of the current operating point of the PV system is positive (e.g., point I with $R_I > 0$), the operation point moves toward the left-side of the PV curve [i.e., point ① in 4(a)]. The algorithm moves the operation point to a point with smaller

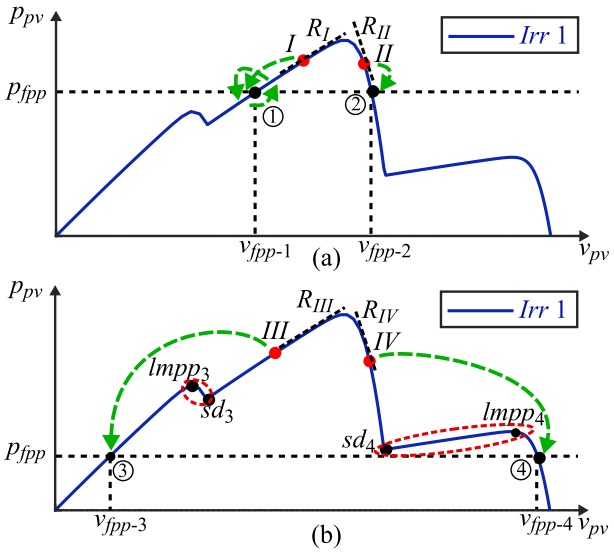

Fig. 4. Principles of CPC operation under partial shading conditions with PV power larger than the reference: (a) Power reference between the section divider point and the current operating point, and (b) power reference smaller than the section divider point power.

power than p_{fpp} as follows:

$$\begin{cases} R > 0, & v_{\text{fpp}} = v_{\text{pv}} - V_{\text{step}} \\ R < 0, & v_{\text{fpp}} = v_{\text{pv}} + V_{\text{step}} \end{cases} \tag{1}$$

in which, $v_{\text{pv–ref}}$ is the PV voltage reference fed to the dc–dc converter voltage control (refer to Fig. 3), v_{pv} is the PV voltage at the current operating point and V_{step} is the voltage step used in the algorithm. The following guidelines can be considered for the selection of the voltage step V_{step} value: i) Selection of relatively large values for V_{step} results in faster dynamics, as the operating point can reach the power reference with smaller number of voltage steps. However, relatively large voltage step values can result in large voltage oscillations during the steady state. ii) On the other hand, small voltage step values result in slow dynamics. On a positive side, small voltage step values lead to relatively small power oscillations at steady state. An adaptive voltage step calculation, similar to the one in [34], can also be applied to enhance both dynamic and steady-state performances. In this case, the operation point moves toward the left-side of the PV curve, until the PV power is smaller than p_{fpp}. Afterward, since p_{pv} is smaller than p_{fpp}, the PV power needs to be increased. This aim can be obtained by using an MPPT algorithm that moves the operation point toward the corresponding local maximum power point (LMPP). In this article, incremental conductance (IC) MPPT algorithm is used [13], [14].

The flowchart of the proposed GFPPT algorithm with CPC functionality is shown in Fig. 5. Assuming no environmental changes are detected (the case with environmental changes will be explained later in the manuscript) and $p_{\text{pv}} > p_{\text{fpp}}$, the operation mode (Mod) is set to 1 (the operation mode is used in the modified GMPP algorithm and will be discussed later in the manuscript). As mentioned, the algorithm should be implemented in such a way that if $R_I > 0$, the operation moves

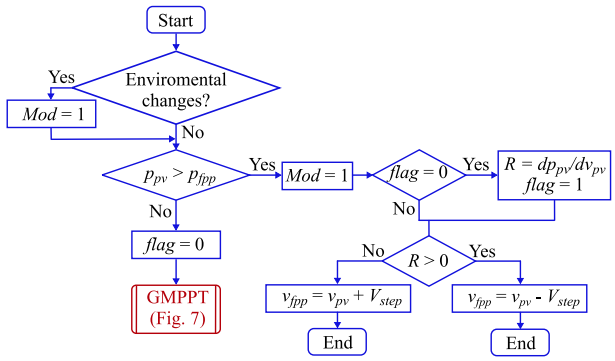

Fig. 5. Proposed GFPPT algorithm with CPC functionality under partial shading conditions.

toward the left-side of the PV curve. For this aim, a variable flag is used in the algorithm. Initially flag is set to zero (flag $= 0$). In this case, the slope of the PV curve is calculated ($R = dp_v/dv_{\text{pv}}$) and the value of flag is set to 1 (flag $= 1$). Subsequently, the operation moves toward the left- or right-side the PV curve based on the sign of R, as in (1).

The importance of using the flag variable is demonstrated in Fig. 4(b). In this case, during the movement of operation point from III to ③, there is a section divider (refer as sd_3). The slope of the PV curve between sd_3 and the its corresponding LMPP (lmpp_3), is negative. If flag is not used, the algorithm becomes stuck at this section divider point (sd_3), because the sign of R changes at this point and the algorithm continues to oscillate around this point. However, since flag is set to 1 at the first instance that $p_{\text{pv}} > p_{\text{fpp}}$, the value and sign of R is only calculated at that instance and in this way, the algorithms continues moving the operation point to the left-side (assuming $R > 0$) until p_{pv} is smaller than p_{fpp}.

As illustrated in Fig. 5, if $p_{\text{pv}} < p_{\text{fpp}}$, the algorithm operates under GMPPT mode to increase the PV power toward the reference. Various cases are demonstrated in Fig. 6 for this operation, as follows.

1) *Corresponding LMPP satisfies the power reference:* As depicted in Fig. 5, at the instance that p_{pv} becomes smaller than p_{fpp}, the parameter flag is set to zero and the operation mode of the GMPPT is Mod $= 1$. Accordingly, the modified GMPPT algorithm is used to increase the power toward** the reference. The flowchart of the modified GMPPT algorithm is illustrated in Fig. 7. It consists of five operation modes. The details of the this search-skip-judge GMPPT algorithm can be found in [45]. The main modification to this GMPPT algorithm is adding the operation mode (Mod). The main purpose of such a modification is that any time that the CPC algorithm moves to GMPPT operation, the algorithm first finds the LMPP, corresponding to the current operation mode. If the corresponding LMPP can satisfy the power reference, as demonstrated in Fig. 6(a), it is not required to skip the voltage reference to the beginning of the PV voltage search range. As shown in Fig. 7, since Mod is equal to 1 at the first instance that the algorithm moves to GMPPT operation, the IC MPPT algorithm is used to calculate the voltage reference.

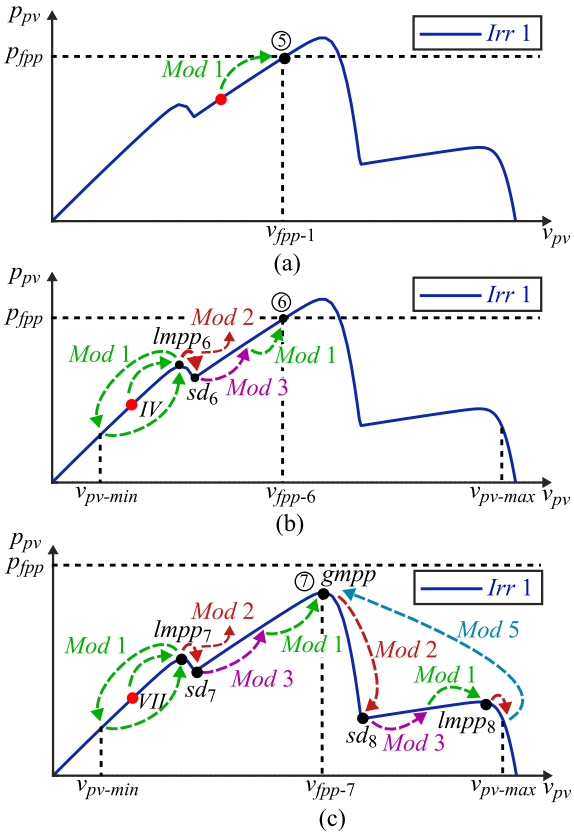

Fig. 6. Principles of GMPP operation under partial shading conditions with PV power smaller than the reference: (a) Power reference between the corresponding LMPP and the current operating point, and (b) power reference larger than the corresponding LMPP, and (c) power reference larger than the GMPP.

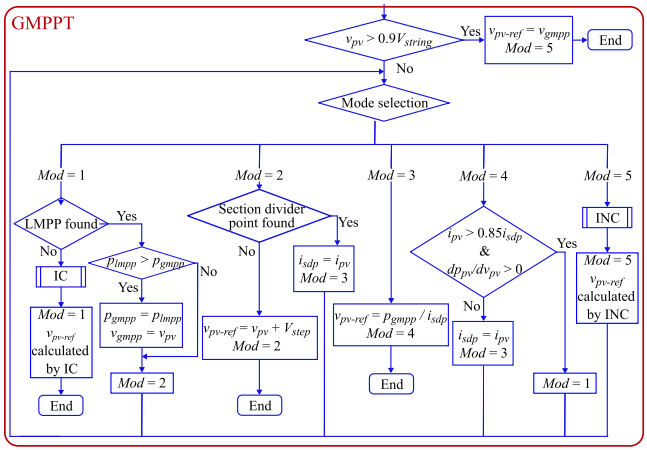

Fig. 7. Flowchart of the modified GMPPT algorithm for the GFPPT operation under partial shading conditions.

2) *Corresponding LMPP does not satisfy the power reference:* As illustrated in Fig. 6(b), the corresponding LMPP to the point IV does not satisfy the power reference. Accordingly, the GMPPT algorithm moves the operation point to the beginning of the voltage search range ($v_{\text{pv-min}}$). Subsequently, the first LMPP (lmpp_6) is found and Mod changes to 2 to find the first section divider (sd_6). Subsequently, the operation mode changes to Mod $= 3$ in order to jump the voltage to $v_{\text{pv-ref}} = p_{\text{gmpp6}}/i_{\text{isdp6}}$. After checking the new operation point in Mod 4, the algorithm goes to Mod 1 to find the next LMPP. As demonstrated in Fig. 6(b), before reaching the next LMPP, the algorithm satisfies the power reference at point ⑥.

3) *Power reference larger than the GMPP:* As shown in Fig. 6(c), the full scan of the PV curve is required in this case and operation point stays at the GMPP (point ⑦) in this case.

The algorithm in [34] is applied for the detection of environmental changes. As shown in Fig. 5, if environmental changes are detected, the operation mode is set to Mod $= 1$. In this case, before changing the voltage to the $v_{\text{pv-min}}$ at the beginning of the search range, the corresponding LMPP is found. The importance of this operation is highlighted in the experimental results Cases I and II.

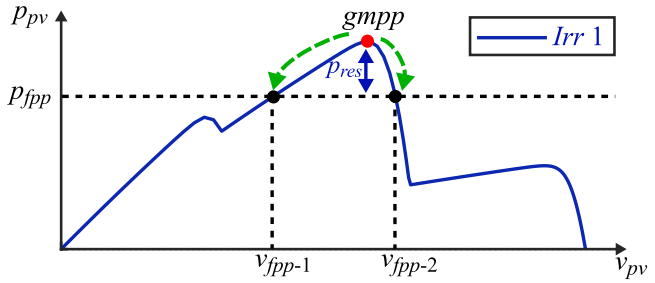

Fig. 8. Principles of the proposed GFPPT algorithm with PRC functionality.

C. Proposed GFPPT Algorithm With PRC Functionality

The principles of the proposed GFPPT algorithm with PRC functionality are illustrated in Fig. 8. The main difference of the PRC functionality to CPC is keeping a predefined power reserve p_{res} in this case. The information of the global maximum power should always be known in order to calculate the reference. The power reference is calculated as

$$p_{\text{fpp}} = p_{\text{gmpp}} - p_{\text{res}} \tag{2}$$

in which, p_{gmpp} is the measured power of the GMPP and p_{res} is the power reserve in the PV system. The flowchart of this algorithm is shown in Fig. 9. After detection of any environmental changes, the GMPPT operation is performed to find the new GMPP power. Once the GMPP is found, the power reference p_{fpp} is calculated. Based on the chosen operation side (left- or right-side of the GMPP), the voltage corresponding power reference is calculated to reduce the PV power to p_{fpp}.

Remark: It is noted that the proposed GFPPT algorithm is applicable to partially shaded PV curves with any number of LMPPs. There is no requirement of any modifications in the algorithm to adapt the proposed algorithm to PV curves with multiple LMPPs. Only for the sake of simplicity, the explanations in this section are provided using PV curves with three LMPPs.

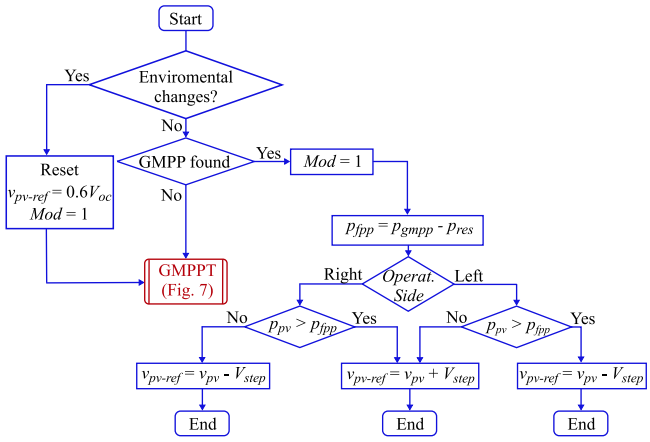

Fig. 9. Proposed GFPPT algorithm with PRC functionality under partial shading conditions.

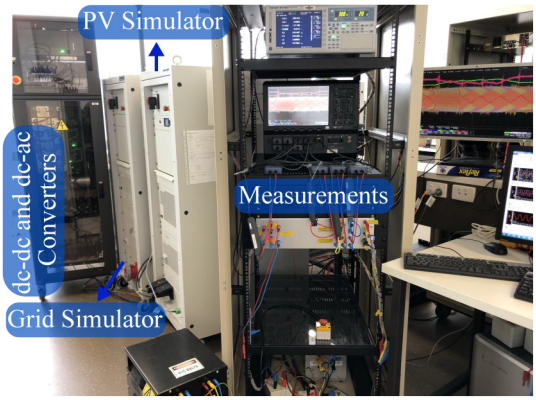

Fig. 10. Picture of the experimental setup.

III. Experimental Results

The performance of the proposed GFPPT algorithms under partial shading conditions is evaluated experimentally on a 2.5-kW two-stage DPV system, as shown in Fig. 3. A three-level neutral-point-clamped inverter is used to connect the PV system to the grid. The proposed GFPPT algorithm is applied to the dc–dc converter, as shown in Fig. 3. The grid is simulated using a Regatron TCACS 4-quadrant grid simulator and the PV is emulated using a Regatron TopCon Quadro programmable dc power supply. The dc supply is equipped with "solar array simulation software" to emulate the behavior of solar array. It can also emulate transitioning PV curves to emulate environmental changes. The proposed controller and protection functions of the converter are implemented in a dSPACE 1006 platform. A picture of the experimental setup is illustrated in Fig. 10 and the parameters of the converter are given in Table II. The performance of the proposed GFPPT algorithms is investigated under four case studies of CPC and PRC.

Two of these case studies investigate the performance of the proposed GFPPT algorithm under irradiance changes to provide constant power. In Case I, the new LMPP can satisfy the power reference, while in Case II, a GMPP scanning is needed to satisfy the required power reference. In the Case III, the performance of the proposed GFPPT algorithm for CPC

TABLE II
Experimental Parameters

Parameter	Value
PV string maximum power, p_{mpp}	2.5 kW
PV string *MPP* voltage, v_{mpp}	275 V
Grid voltage (line-neutral, rms), $v_{g\text{-}ln}$	110 V
Grid frequency, f	50 Hz
Grid connection inductor filter, L_f	9 mH

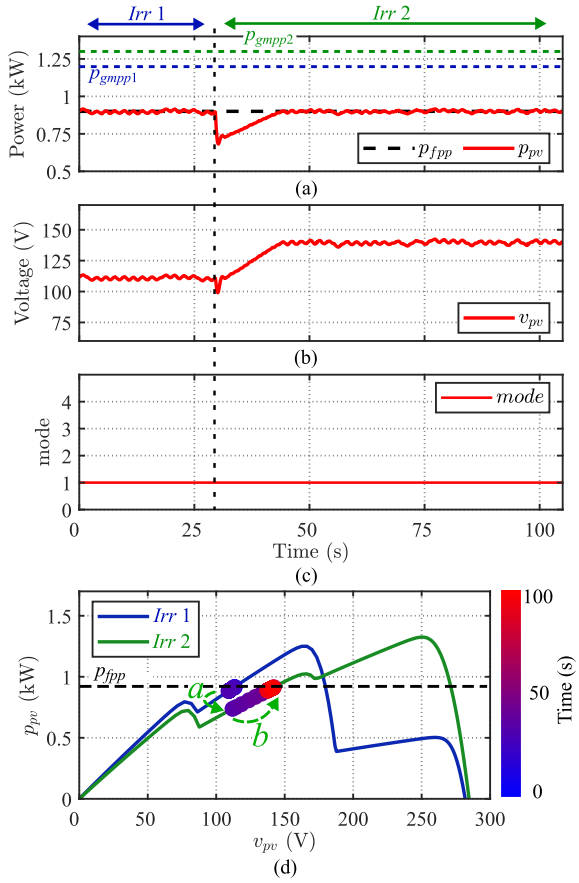

Fig. 11. Case I—Experimental results of the proposed GFPPT algorithm with CPC functionality under changing partial shading conditions (LMPP satisfies the power reference): (a) PV voltage, (b) PV power, (c) operation mode, and (d) P–V operation point.

operation under step change of the power reference is investigated. Finally, the performance for PRC control under changing irradiance conditions is investigated in Case IV. Together, these case studies demonstrate that the proposed GFPPT algorithm is able to provide the required CPC or PRC features in PV systems under various possible operating conditions.

Case I—CPC under changing partial shading conditions (LMPP satisfies the power reference): At the beginning of this case study, the irradiance is Irr 1 with $p_{\text{gmpp1}} = 1.25\,\text{kW}$. A power reference of $p_{\text{fpp}} = 0.9\,\text{kW}$ is considered in this case study. The results are shown in Fig. 11. Before $t = 30\,\text{s}$, the PV power is regulated at the reference by regulating its voltage at 110 V, as shown in Fig. 11(a) and (b). The control operation

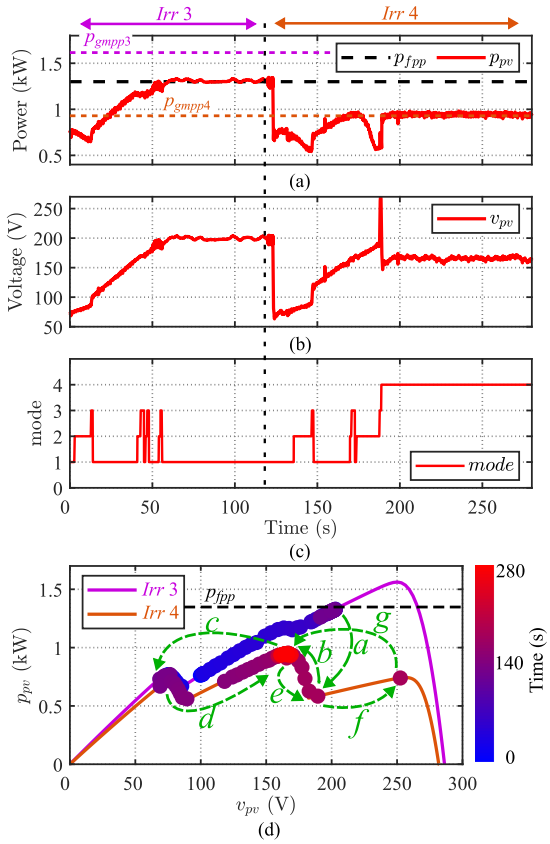

Fig. 12. Case II—Experimental results of the proposed GFPPT algorithm with CPC functionality under changing partial shading conditions (GMPP scanning is required): (a) PV voltage, (b) PV power, (c) operation mode, and (d) P–V operation point.

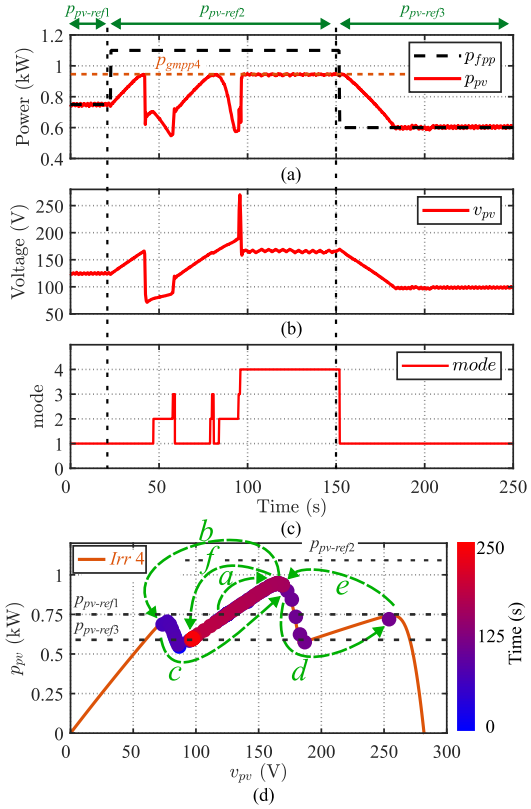

Fig. 13. Case III—Experimental results of the proposed GFPPT algorithm with CPC functionality under changing PV power reference: (a) PV voltage, (b) PV power, (c) operation mode, and (d) P–V operation point.

mode is 1 (mode $= 1$) during this period, which means the PV operates at the LMPP mode.

At $t = 30$ s, the irradiance changes to Irr 2, which corresponds to GMPP power of 1.3 kW at $v_{\text{gmpp}} = 250$ V. As shown in Fig. 11(c), the operation mode after the irradiance remains at mode $= 1$. As discussed in Section II, after detection of any environmental changes, the algorithm stays at LMPP operation mode (mode $= 1$) until the LMPP is found. This case study highlights the benefit of this operation mode, because after the irradiance change in this case, the PV power reference lies within the new LMPP region of the new P–V curve, as illustrated in Fig. 11(d). Under this case, the PV operation point does not need to reset to the beginning of the search region, which leads to faster dynamics in tracking the power reference.

Case II—CPC under changing partial shading conditions (GMPP scanning is required): At the beginning of this case study, the PV system has irradiance of Irr 3, corresponding to GMPP of $p_{\text{gmpp3}} = 1.6$ kW. The irradiance changes from Irr 3 to Irr 4 at $t = 125$ s. The GMPP of the new PV curve ($p_{\text{gmpp4}} = 0.96$ kW) is smaller than the power reference $p_{\text{fpp}} = 1.25$ kW, as shown in Fig. 12. It is seen in Fig. 12(c) that the operation mode stays at mode $= 1$ after the irradiance change to check whether the corresponding new LMPP can satisfy the power reference or not.

During this period, the operation point moves along arrow b in Fig. 12(d). Unlike Case I, the LMPP does not satisfy the power reference. Accordingly, the algorithm resets the PV voltage to the beginning of the voltage search range $v_{\text{pv}} = 75$ V (along arrow c). After finding the LMPP, the operation mode changes to mode $= 2$ to find the section divider (following arrow d). Subsequently, the algorithm scans the curve until the end of the search region (following arrows e and f). Finally, the proposed algorithm moves the operation point to the GMPP ($v_{\text{pv}} = 170$ V and $p_{\text{pv}} = 0.96$ kW) and operation modes changes to mode $= 4$, as illustrated in Fig. 12(c). This case study highlights the performance of the proposed GFPPT algorithm to operate the PV system at GMPP, if the power reference is larger than the GMPP power.

Case III—CPC under changing PV power reference condition: A step increase and decrease of the power reference is tested in this case study. The performance of the proposed GFPPT algorithm in regulating the PV power to the new reference is investigated. The results are shown in Fig. 13. The PV curve with Irr 4 has a GMPP power of $p_{\text{gmpp4}} = 0.96$ kW. Before $t = 25$ s, the power reference is set to $p_{\text{fpp}} = 0.75$ kW and the proposed GFPPT algorithm regulates the power by regulating the PV voltage to $v_{\text{pv}} = 125$ V.

At $t = 25$ s, the power reference changes to $p_{\text{fpp}} = 1.1$ kW, which is larger than the GMPP power. Accordingly the proposed GFPPT algorithm scans the PV curve following arrows a, b, c, d, e, shown in Fig. 13(d) to find the GMPP. It stays

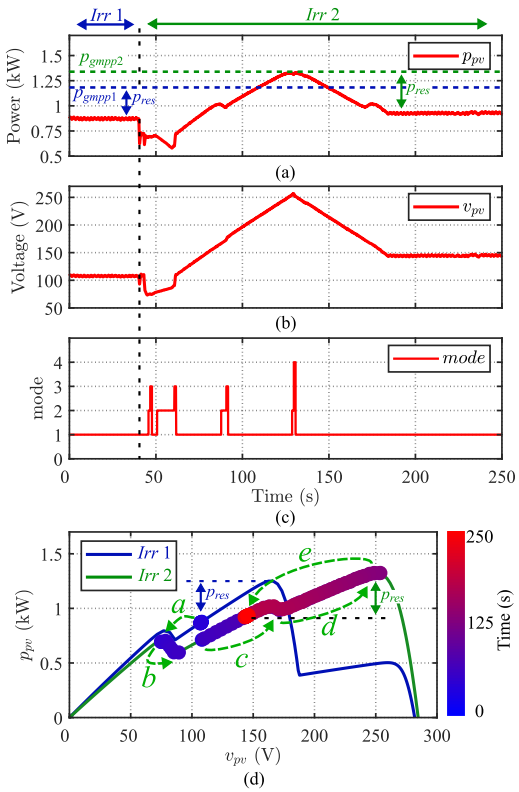

Fig. 14. Case IV—Experimental results of the proposed GFPPT algorithm with PRC functionality under changing partial shading conditions: (a) PV voltage, (b) PV power, (c) operation mode, and (d) P–V operation point.

at this point by operating at mode $= 4$, until the power reference changes. At $t = 150\,\mathrm{s}$ the power reference changes to $p_{\mathrm{fpp}} = 0.6\,\mathrm{kW}$. Accordingly, the proposed algorithm regulates the PV power by reducing the voltage following arrow f. This case study highlights that if the power reference reduces, the proposed algorithm can simply regulate the PV power by simply reducing the PV voltage, without the need of scanning the whole P–V voltage range.

Case IV—PRC under changing partial shading condition: The GFPPT algorithm operates with PRC functionality with a power reserve of 30% ($p_{\mathrm{res}} = 0.3 p_{\mathrm{gmpp}}$) in this case study. The results under changing irradiance condition are illustrated in Fig. 14. Before $t = 40\,\mathrm{s}$, the irradiance is Irr 1 with $p_{\mathrm{gmpp1}} = 1.25\,\mathrm{kW}$. It is clear that the PV power is regulated to $p_{\mathrm{pv}} = 0.88\,\mathrm{kW}$ during this period to provide the power reserve of 30%. At $t = 40\,\mathrm{s}$, the irradiance changes to Irr 2 with $p_{\mathrm{gmpp1}} = 1.4\,\mathrm{kW}$ at $v_{\mathrm{gmpp2}} = 250\,\mathrm{V}$. As mentioned in Section II-C, under PRC operation, after detection of any environmental changes, a GMPP scanning is performed to detect the new global maximum power. In this case, the operation point moves to the beginning of voltage search range, following arrow a and subsequently the GMPP is found by moving the operation point aligned arrows b, c, and d in Fig. 14. Finally, to provide the power reserve of 30%, the operation point moves to the left-side of GMPP, following arrow e. This test demonstrates the desired performance of the proposed GFPPT algorithm with PRC functionality under environmental changes.

IV. Discussion

The speed of the convergence of the proposed GFPPT algorithm depends on several factors.

1) *The operation mode of the algorithm:* As outlined in Section II, based on the power reference and current operating point of the PV curve, different scenarios may occur. In some operation modes, the algorithm requires only a few iterations to regulate the power to the reference (see Fig. 11, the period between $t = 30\,\mathrm{s}$ and $t = 40\,\mathrm{s}$). However, under some conditions, such as the case that requires finding the GMPP, a relatively long convergence time is required (for instance, see Fig. 12, the period between $t = 125\,\mathrm{s}$ and $t = 200\,\mathrm{s}$, that the scan of the whole P–V curve has occurred).
2) *The voltage step V_{step} used in the algorithm:* As mentioned in Section II, there is a tradeoff between the selection of the voltage step for the steady-state oscillations and dynamic performance. For the sake of simplicity, a constant voltage step is considered in the implementation of the proposed GFPPT algorithm. The value of the voltage step has an important effect in the speed of the convergence, because as shown in the flowchart Fig. 7, the voltage step is used to perturb the voltage and power under several operating modes. The effect of using a fixed V_{step} can be clearly seen in the experimental result of Fig. 11, the period between $t = 30\,\mathrm{s}$ and $t = 40\,\mathrm{s}$. It is seen that the voltage is linearly changed in this condition. As a future research direction, using variable or adaptive voltage step, such as the one in [34], can enhance the speed of the convergence.
3) *The time-step T_{step} of the execution of the algorithm:* The execution of the proposed GFPPT algorithm is performed on a discrete domain with constant time step. The operation principle is based on the perturbation of the voltage reference and decision on the next step, based on the corresponding change of the PV power. In this case, the time step for GFPPT execution should be selected long enough to ensure that the "dc–dc converter voltage control" in Fig. 3 is able to regulate the PV voltage to the new reference, before the next execution time. Accordingly, with a fast voltage control loop, and using a higher switching frequency and more advanced voltage controller (such as model predictive control, etc.) a relatively faster convergence time can be obtained [51].

V. Conclusion

A GFPPT algorithm for PV systems under partial shading conditions has been proposed in this article. The algorithm provides two functionalities, i.e., CPC and PRC, which are required for frequency support in PV systems. The conventional search-skip-judge GMPPT algorithm is modified to adapt the proposed GFPPT algorithm. The performance of the proposed GFPPT algorithm has also been investigated experimentally under various operating conditions, including irradiance sudden changes and power reference changes.

REFERENCES

[1] H. Li, D. Yang, W. Su, J. Lü, and X. Yu, "An overall distribution particle swarm optimization MPPT algorithm for photovoltaic system under partial shading," *IEEE Trans. Ind. Electron.*, vol. 66, no. 1, pp. 265–275, Jan. 2019.

[2] X. Li, H. Wen, Y. Hu, Y. Du, and Y. Yang, "A comparative study on photovoltaic MPPT algorithms under EN50530 dynamic test procedure," *IEEE Trans. Power Electron.*, vol. 36, no. 4, pp. 4153–4168, Apr. 2021.

[3] K. Y. Yap, C. R. Sarimuthu, and J. M. Y. Lim, "Artificial intelligence based MPPT techniques for solar power system: A review," *J. Modern Power Syst. Clean Energy*, vol. 8, no. 6, pp. 1043–1059, Nov. 2020.

[4] S. Motahhir, A. El Hammoumi, and A. El Ghzizal, "The most used MPPT algorithms: Review and the suitable low-cost embedded board for each algorithm," *J. Cleaner Prod.*, vol. 246, 2020, Art. no. 118983.

[5] M. M. Haque and P. Wolfs, "A review of high PV penetrations in LV distribution networks: Present status, impacts and mitigation measures," *Renewable Sustain. Energy Rev.*, vol. 62, pp. 1195–1208, 2016.

[6] K. Ndirangu, H. Dehghani Tafti, J. E. Fletcher, and G. Konstantinou, "Impact of grid voltage and grid-supporting functions on efficiency of single-phase photovoltaic inverters," *IEEE J. Photovolt.*, vol. 12, no. 1, pp. 421–428, Jan. 2022.

[7] Australia/New Zealand Standard AS/NZS 4777.2, "Grid-connected PV systems: Design and installation training manual," Dec. 2020. [Online]. Available: https://www.standards.org.au/standards-catalogue/sa-snz/electrotechnology/el-042/as-slash-nzs-4777-dot-2-colon-2020

[8] *IEEE Recommended Practice for Interconnecting Distributed Resources With Electric Power Systems Distribution Secondary Networks*, IEEE Std 1547, Apr. 2018.

[9] H. D. Tafti *et al.*, "Extended functionalities of photovoltaic systems with flexible power point tracking: Recent advances," *IEEE Trans. Power Electron.*, vol. 35, no. 9, pp. 9342–9356, Sep. 2020.

[10] V. Kamala Devi, K. Premkumar, A. Bisharathu Beevi, and S. Ramaiyer, "A modified perturb & observe MPPT technique to tackle steady state and rapidly varying atmospheric conditions," *Sol. Energy*, vol. 157, pp. 419–426, 2017.

[11] M. Killi and S. Samanta, "Modified perturb and observe MPPT algorithm for drift avoidance in photovoltaic systems," *IEEE Trans. Ind. Electron.*, vol. 62, no. 9, pp. 5549–5559, Sep. 2015.

[12] A. Safari and S. Mekhilef, "Simulation and hardware implementation of incremental conductance MPPT with direct control method using Cuk converter," *IEEE Trans. Ind. Electron.*, vol. 58, no. 4, pp. 1154–1161, Apr. 2011.

[13] F. Liu, S. Duan, F. Liu, B. Liu, and Y. Kang, "A variable step size INC MPPT method for PV systems," *IEEE Trans. Ind. Electron.*, vol. 55, no. 7, pp. 2622–2628, Jul. 2008.

[14] H. Shahid, M. Kamran, Z. Mehmood, M. Y. Saleem, M. Mudassar, and K. Haider, "Implementation of the novel temperature controller and incremental conductance MPPT algorithm for indoor photovoltaic system," *Sol. Energy*, vol. 163, pp. 235–242, Mar. 2018.

[15] Y.-P. Huang and S.-Y. Hsu, "A performance evaluation model of a high concentration photovoltaic module with a fractional open circuit voltage-based maximum power point tracking algorithm," *Comput. Elect. Eng.*, vol. 51, pp. 331–342, Apr. 2016.

[16] H. A. Sher, A. F. Murtaza, A. Noman, K. E. Addoweesh, K. Al-Haddad, and M. Chiaberge, "A new sensorless hybrid MPPT algorithm based on fractional short-circuit current measurement and P&O MPPT," *IEEE Trans. Sustain. Energy*, vol. 6, no. 4, pp. 1426–1434, Oct. 2015.

[17] M. Ricco, P. Manganiello, E. Monmasson, G. Petrone, and G. Spagnuolo, "FPGA-based implementation of dual Kalman filter for PV MPPT applications," *IEEE Trans. Ind. Informat.*, vol. 13, no. 1, pp. 176–185, Feb. 2017.

[18] B. N. Alajmi, K. H. Ahmed, S. J. Finney, and B. W. Williams, "Fuzzy-logic-control approach of a modified hill-climbing method for maximum power point in microgrid standalone photovoltaic system," *IEEE Trans. Power Electron.*, vol. 26, no. 4, pp. 1022–1030, Apr. 2011.

[19] A. El Khateb, N. A. Rahim, J. Selvaraj, and M. N. Uddin, "Fuzzy-logic-controller-based SEPIC converter for maximum power point tracking," *IEEE Trans. Ind. Appl.*, vol. 50, no. 4, pp. 2349–2358, Jul./Aug. 2014.

[20] N. Priyadarshi, V. K. Ramachandaramurthy, S. Padmanaban, and F. Azam, "An ant colony optimized MPPT for standalone hybrid PV-wind power system with single cuk converter," *Energies*, vol. 12, no. 1, Jan. 2019, Art. no. 167.

[21] H.-D. Liu, C.-H. Lin, K.-J. Pai, and Y.-L. Lin, "A novel photovoltaic system control strategies for improving hill climbing algorithm efficiencies in consideration of radian and load effect," *Energy Convers. Manage.*, vol. 165, pp. 815–826, Jun. 2018.

[22] X. Li, H. Wen, L. Jiang, W. Xiao, Y. Du, and C. Zhao, "An improved MPPT method for PV system with fast-converging speed and zero oscillation," *IEEE Trans. Ind. Appl.*, vol. 52, no. 6, pp. 5051–5064, Nov./Dec. 2016.

[23] V. V. R. Scarpa, S. Buso, and G. Spiazzi, "Low-complexity MPPT technique exploiting the PV odule MPP locus characterization," *IEEE Trans. Ind. Electron.*, vol. 56, no. 5, pp. 1531–1538, May 2009.

[24] C. Rosa, D. Vinikov, E. Romero-Cadaval, V. Pires, and J. Martins, "Low-power home PV systems with MPPT and PC control modes," in *Proc. Int. Conf. Workshop Compat. Power Electron.*, 2013, pp. 58–62.

[25] S. M. Park and S. Y. Park, "Power weakening control of the photovoltaic-battery system for seamless energy transfer in microgrids," in *Proc. Appl. Power Electron. Conf.*, pp. 2971–2976, 2013.

[26] Y. Yang, H. Wang, F. Blaabjerg, and T. Kerekes, "A hybrid power control concept for PV inverters with reduced thermal loading," *IEEE Trans. Power Electron.*, vol. 29, no. 12, pp. 6271–6275, Dec. 2014.

[27] H. D. Tafti, C. D. Townsend, G. Konstantinou, and J. Pou, "A multi-mode flexible power point tracking algorithm for photovoltaic power plants," *IEEE Trans. Power Electron.*, vol. 34, no. 6, pp. 5038–5042, Jun. 2019.

[28] H. Tafti, A. Maswood, G. Konstantinou, J. Pou, and P. Acuna, "Active/reactive power control of photovoltaic grid-tied inverters with peak current limitation and zero active power oscillation during unbalanced voltage sags," *IET Power Electron.*, vol. 11, no. 6, pp. 1066–1073, May 2018.

[29] H. D. Tafti, A. I. Maswood, J. Pou, G. Konstantinou, and V. G. Agelidis, "An algorithm for reduction of extracted power from photovoltaic strings in grid-tied photovoltaic power plants during voltage sags," in *Proc. Annu. Conf. IEEE Ind. Electron. Soc.*, pp. 3018–3023, 2016.

[30] Y. Yang, E. Koutroulis, A. Sangwongwanich, and F. Blaabjerg, "Pursuing photovoltaic cost-effectiveness: Absolute active power control offers hope in single-phase PV systems," *IEEE Ind. Appl. Mag.*, vol. 23, no. 5, pp. 40–49, Jun. 2017.

[31] A. Sangwongwanich, Y. Yang, F. Blaabjerg, and D. Sera, "Delta power control strategy for multistring grid-connected PV inverters," *IEEE Trans. Ind. Appl.*, vol. 53, no. 4, pp. 3862–3870, Jul. 2017.

[32] H. D. Tafti, A. I. Maswood, G. Konstantinou, J. Pou, and F. Blaabjerg, "A general constant power generation algorithm for photovoltaic systems," *IEEE Trans. Power Electron.*, vol. 33, no. 5, pp. 4088–4101, May 2018.

[33] H. D. Tafti, A. Sangwongwanich, Y. Yang, G. Konstantinou, J. Pou, and F. Blaabjerg, "A general algorithm for flexible active power control of photovoltaic systems," in *Proc. Appl. Power Electron. Conf.*, 2018, pp. 1115–1121.

[34] H. Dehghani Tafti, A. Sangwongwanich, Y. Yang, J. Pou, G. Konstantinou, and F. Blaabjerg, "An adaptive control scheme for flexible power point tracking in photovoltaic systems," *IEEE Trans. Power Electron.*, vol. 34, no. 6, pp. 5451–5463, Jun. 2019.

[35] R. Gomez-Merchan *et al.*, "Binary search-based flexible power point tracking algorithm for photovoltaic systems," *IEEE Trans. Ind. Electron.*, vol. 68, no. 7, pp. 5909–5920, Jul. 2021.

[36] A. Kumaresan, H. Dehghani Tafti, K. Nandha Kumar, G. G. Farivar, J. Pou, and T. Subbaiyan, "Flexible power point tracking for solar photovoltaic systems using secant method," *IEEE Trans. Power Electron.*, vol. 36, no. 8, pp. 9419–9429, Aug. 2021.

[37] Y. Ji, D. Jung, J. Kim, J. Kim, T. Lee, and C. Won, "A real maximum power point tracking method for mismatching compensation in PV array under partially shaded conditions," *IEEE Trans. Power Electron.*, vol. 26, no. 4, pp. 1001–1009, Apr. 2011.

[38] K. S. Tey and S. Mekhilef, "Modified incremental conductance algorithm for photovoltaic system under partial shading conditions and load variation," *IEEE Trans. Ind. Electron.*, vol. 61, no. 10, pp. 5384–5392, Oct. 2014.

[39] R. B. A. Koad, A. F. Zobaa, and A. El-Shahat, "A novel MPPT algorithm based on particle swarm optimization for photovoltaic systems," *IEEE Trans. Sustain. Energy*, vol. 8, no. 2, pp. 468–476, Apr. 2017.

[40] L. Guo, Z. Meng, Y. Sun, and L. Wang, "A modified cat swarm optimization based maximum power point tracking method for photovoltaic system under partially shaded condition," *Energy*, vol. 144, pp. 501–514, Feb. 2018.

[41] S. Mohanty, B. Subudhi, and P. K. Ray, "A new MPPT design using grey wolf optimization technique for photovoltaic system under partial shading conditions," *IEEE Trans. Sustain. Energy*, vol. 7, no. 1, pp. 181–188, Jan. 2016.

[42] C. Manickam, G. R. Raman, G. P. Raman, S. I. Ganesan, and C. Nagamani, "A hybrid algorithm for tracking of GMPP based on P&O and PSO with reduced power oscillation in string inverters," *IEEE Trans. Ind. Electron.*, vol. 63, pp. 6097–6106, Oct. 2016.

[43] A. Ibrahim, S. Obukhov, and R. Aboelsaud, "Determination of global maximum power point tracking of PV under partial shading using cuckoo search algorithm," *Appl. Sol. Energy*, vol. 55, pp. 367–375, 2019.
[44] B. Peng, K. Ho, and Y. Liu, "A novel and fast MPPT method suitable for both fast changing and partially shaded conditions," *IEEE Trans. Ind. Electron.*, vol. 65, no. 4, pp. 3240–3251, Apr. 2018.
[45] Y. Wang, Y. Li, and X. Ruan, "High-accuracy and fast-speed MPPT methods for PV string under partially shaded conditions," *IEEE Trans. Ind. Electron.*, vol. 63, no. 1, pp. 235–245, Jan. 2016.
[46] E. I. Batzelis, S. A. Papathanassiou, and B. C. Pal, "PV system control to provide active power reserves under partial shading conditions," *IEEE Trans. Power Electron.*, vol. 33, no. 11, pp. 9163–9175, Nov. 2018.
[47] P. Verma, T. Kaur, and R. Kaur, "Power control strategy of PV system for active power reserve under partial shading conditions," *Int. J. Elect. Power Energy Syst.*, vol. 130, Sep. 2021, Art. no. 106951.
[48] Z. Xie and Z. Wu, "A flexible power point tracking algorithm for photovoltaic system under partial shading condition," *Sustain. Energy Technol. Assessments*, vol. 49, Feb. 2022, Art. no. 101747.
[49] H. D. Tafti, G. Konstantinou, J. Fletcher, L. Callegaro, G. G. Farivar, and J. Pou, "Control of distributed photovoltaic inverters for frequency support and system recovery," *IEEE Trans. Power Electron.*, vol. 37, no. 4, pp. 4742–4750, Apr. 2022.
[50] Y. Su *et al.*, "An adaptive PV frequency control strategy based on real-time inertia estimation," *IEEE Trans. Smart Grid*, vol. 12, no. 3, pp. 2355–2364, May 2021.
[51] A. Narang *et al.*, "An algorithm for fast flexible power point tracking in photovoltaic power plants," in *Proc. 45th Annu. Conf. IEEE Ind. Electron. Soc.*, vol. 1, pp. 4387–4392, Oct. 2019.

Hossein Dehghani Tafti (Senior Member, IEEE) received the B.Sc. and M.Sc. degrees in electrical engineering and power system engineering from the Amirkabir University of Technology, Tehran, Iran, in 2009 and 2011, respectively, and the Ph.D. degree in electrical engineering from Nanyang Technological University, Singapore, in 2018.

From January 2018 to April 2020, he was a Research Fellow with Nanyang Technological University, where he was working on the control of photovoltaic systems for grid support. From May 2020 to May 2021, he was a Senior Research Associate with the University of New South Wales, Sydney, NSW, Australia, where he worked on modeling and testing of commercial photovoltaic inverters. He is currently a Research Fellow with the Department of Electrical, Electronic and Computer Engineering, University of Western Australia, Perth, WA, Australia. He was the Co-Editor of the book titled *Advanced Multilevel Converters and Applications in Grid Integration* (Wiley, 2018). His research interest includes the grid-integration of renewable energy sources, in particular, photovoltaics and energy storage, and design and control of multilevel power converters.

Qijun Wang received the B.Eng. and M.Eng. degrees in electrical engineering and photovoltaics from the University of New South Wales, Sydney, NSW, Australia, in 2021.

From February 2020 to December 2021, he was working on the control of photovoltaic systems for grid support. He is currently a Technical Engineer with One Stop Warehouse, Australia's largest solar distributor, Crestmead, QLD, Australia.

Christopher D. Townsend (Member, IEEE) received the B.E. and Ph.D. degrees in electrical engineering from the University of Newcastle, Callaghan, NSW, Australia, 2009 and 2013, respectively.

Subsequently, he spent three years working with ABB Corporate Research, Västerås, Sweden, working on next-generation high-power converter technologies. Since then he has held various postdoctoral research positions including with the University of New South Wales, Sydney, NSW, Australia, the University of Newcastle, and Nanyang Technological University, Singapore. In 2019, he joined the Department of Electrical, Electronic and Computer Engineering, The University of Western Australia, Perth, WA, Australia, as a Senior Lecturer. He has authored more than 60 published technical papers and has been involved in several industrial projects and educational programs in the field of power electronics. His research interests include topologies and modulation strategies for multilevel converters applied in power systems, renewable energy integration, and electric vehicle applications.

Dr. Townsend is a member of the IEEE POWER ELECTRONICS AND INDUSTRIAL ELECTRONICS SOCIETIES.

Josep Pou (Fellow, IEEE) received the B.S., M.S., and Ph.D. degrees in electrical engineering from the Technical University of Catalonia (UPC)-Barcelona Tech, Barcelona, Spain, in 1989, 1996, and 2002, respectively.

In 1990, he joined the faculty of UPC as an Assistant Professor, where he became an Associate Professor in 1993. From February 2013 to August 2016, he was a Professor with the University of New South Wales (UNSW), Sydney, NSW, Australia. He is currently a Professor with the Nanyang Technological University (NTU), Singapore, where he is a Cluster Director of Power Electronics with the Energy Research Institute at NTU (ERI@N), Singapore, and a Co-Director of the Rolls-Royce at NTU Corporate Lab. From February 2001 to January 2002, and February 2005 to January 2006, he was a Researcher with the Center for Power Electronics Systems, Virginia Tech, Blacksburg, VA, USA. From January 2012 to January 2013, he was a Visiting Professor with the Australian Energy Research Institute, UNSW. He has authored more than 380 published technical papers and has been involved in several industrial projects and educational programs in the fields of power electronics and systems. His research interests include modulation and control of power converters, multilevel converters, renewable energy, energy storage, power quality, HVdc transmission systems, and more-electrical aircraft and vessels.

Dr. Pou is currently an Associate Editor of IEEE JOURNAL OF EMERGING AND SELECTED TOPICS IN POWER ELECTRONICS. He was a Co-Editor-in-Chief and an Associate Editor of IEEE TRANSACTIONS ON INDUSTRIAL ELECTRONICS. He was the recipient of the 2018 IEEE Bimal Bose Award for Industrial Electronics Applications in Energy Systems.

Georgios Konstantinou (Senior Member, IEEE) received the B.Eng. degree in electrical and computer engineering from the Aristotle University of Thessaloniki, Thessaloniki, Greece, in 2007 and the Ph.D. degree in electrical engineering from The University of New South Wales (UNSW Sydney), Sydney, NSW, Australia, in 2012.

From 2013 to 2016, he was a Senior Research Associate with the University of New South Wales, Sydney, NSW, Australia, where he was a part of the Australian Energy Research Institute. Since 2017, he has been with the School of Electrical Engineering and Telecommunications, UNSW Sydney, where he is currently a Senior Lecturer. His main research interests include multilevel converters, power electronics in HVdc renewable energy and energy storage applications.

Dr. Konstantinou is currently an Associate Editor of IEEE TRANSACTIONS ON POWER ELECTRONICS, IEEE TRANASCTIONS ON INDUSTRIAL ELECTRONICS, and *IET Power Electronics*.